High-resolution X-Ray spectral diagnostics of Active Galactic Nuclei

Steenbrugge, K.C.

Chapter 1

Introduction

1.1 Motivation

In the center of most galaxies, even non active galaxies such as our own Milky Way, there is a super massive black hole (SMBH). The masses of these SMBH's range from 10^6 to 10^9 M$_\odot$. The luminosity radiated by the infalling gas depends on its mass and its trajectory in the gravitational potential. In the Milky Way the amount of gas captured by the SMBH is rather limited. The captured gas either belongs to a giant molecular cloud moving near the SMBH; or is accumulated from the outer layers of stars, which have been stripped due to a gravitational interaction with the SMBH. This gas falls into the SMBH without forming an accretion disk. As a result, the emission from our SMBH is barely detectable in most wavelength bands. However, the gravitational potential of our SMBH is traced by the stellar orbits in its vicinity. Using one such stellar orbit Schödel et al. (2002) determined the mass of our SMBH to be $3.7 \pm 1.5 \times 10^6$ M$_\odot$. In contrast, in an Active Galactic Nucleus (AGN) there is a large amount of gas, which presumably forms an accretion disk before spiraling into the SMBH. The observed luminosity of an AGN is in large part due to radiation from the accretion disk.

Using the standard thin disk theory (Shakura & Sunyaev 1973) one can calculate the temperature of the disk as a function of its radius. It is found that most of the energy is radiated at about 3 gravitational radii. The disk spectrum can be approximated by a multi-temperature black body. However, as most of the radiation is emitted from about 3 gravitational radii, the spectrum can also be approximated by a standard black body. This black body spectrum has a peak in the extreme UV/the soft X-ray range of the spectrum. Our Milky Way absorbs the extreme UV radiation, thus the accretion disks

of AGNs are best studied in the soft X-ray regime. Observing AGN in the X-rays we thus study the environment surrounding the SMBH.

1.2 Taxonomy

Active Galactic Nuclei are known under several different names, from classifying timing or spectral characteristics. Although originally all these classes were thought to be objects with different physical properties, more recently they have mostly been unified as due to an active SMBH fed through an accretion disk and producing a pair of jets. In this theory the inclination angle under which we view the AGN explains a number of the different characteristics observed (Antonucci & Miller 1985; Barthel 1989; Urry & Padovani 1995). For instance, blazars which are very variable in the optical have been identified as AGNs in which we look directly into the jet.

A large number of AGN can be classified into two broad classes, the unobscured (Type 1) and obscured (Type 2). The continuum emission of Type 2 AGNs is absorbed by gas and dust in the optical, UV and soft X-ray band and re-radiated in the infrared. Due to inverse-Compton scattering these AGNs are detected in the hard X-ray and soft gamma-ray band. Type 1 AGNs are not, or much less obscured by dust, and are bright in the extreme UV and soft X-rays. A subset of these Type 1 and Type 2 AGNs are the Seyfert galaxies, which are believed to be gas-rich spirals. Spectra of Seyfert 1 galaxies show broad and narrow emission lines; spectra of Seyfert 2 galaxies only show narrow emission lines, when viewed in unpolarized optical light.

Antonucci & Miller (1985) discovered that spectra of Seyfert 2 galaxies show broad emission lines in polarized light. Most of the photons emitted in the broad line region are scattered out of our line of sight by intervening cold gas. However, by suppressing the unscattered continuum with a polarization filter, Antonucci & Miller (1985) detected these broad emission lines. The detection of these broad emission lines in spectra of Seyfert 2 galaxies hinted that Seyfert 1 and Seyfert 2 galaxies have the same physical properties, but that the Seyfert 2 galaxies are obscured (Antonucci & Miller 1985). The source of obscuration is generally thought to be a torus in the equatorial plane.

1.3 Observational facts from X-ray observations

The black body spectrum emitted from the accretion disk, as predicted by the thin disk theory (Shakura & Sunyaev 1973) was already detected in early observations of Seyfert 1 galaxies. These observations also showed that AGNs emit a hard X-ray continuum,

which is modeled as a power-law with a cut-off energy above 100 keV, and is explained by inverse-Compton scattering of UV/soft X-ray photons on hot electrons. These hot electrons are located near the accretion disk and are collectively referred to as the hot corona. A possible location for this hot corona is the inner edge of the accretion disk (e.g. Chakrabarti & Titarchuk 1995).

The power law becomes harder around 10 keV, due to reflection on a dense and lowly ionized gas. Passing through this gas the photons lose energy through Compton scattering and absorption. As a result, the original power-law slope is changed, and appears to become harder at 10 keV. The narrow Fe Kα emission line observed in most Seyfert galaxies is also due to reflection on cold material. In the case of NGC 1068 this cold gas is located less than 2 pc from the nucleus and is unresolved with current infrared interferometry instruments such as MIDI. This observation severely limits possible models for this gas component, as the gas pressure can not support the gas in the strong gravitational field and it should collapse (Röttgering et al. 2004). This dense gas may be located in a torus at the outer edge of the accretion disk. Alternatively, the dense gas is the optically thick accretion disk (Lightman & White 1988; Guilbert & Rees 1988). However, the data are also consistent with a wind that is radiatively driven by dust grain opacity (Königl & Kartje 1994). Another possibility is that the dense gas is in the form of $5 - 10$ large clouds, which are preferentially located in the equatorial plane (Nenkova, Ivezić & Elitzur 2002). Common names for this neutral gas are the inner torus, molecular torus or obscuring torus. I will use the term torus, whether or not it occurs in a torus shape.

Some X-ray observations indicate that there is in addition to the narrow Fe Kα emission line a relativistically broadened Fe Kα emission line (Tanaka et al. 1995; Wilms et al. 2001) formed at the inner edge of the accretion disk. If this line is indeed relativistically broadened then from the line profile we can derive the distance between the inner edge of the accretion disk and the event horizon of the SMBH. From this distance one can determine the radius of the last stable circular orbit and thus the rotational velocity of the black hole. In the well studied case of MGC -6-30-15 the line profile is consistent with a maximally rotating (Kerr) black hole (Iwasawa et al. 1996; Wilms et al. 2001). Also the inclination angle of the accretion disk can be determined from the line profile. This measurement is important as it can discriminate between the different models for the cores of AGN's. Possibly, in the soft X-ray band, relativistically broadened emission lines from O VIII Lyα, N VII Lyα and C VI Lyα are also detected (Branduardi-Raymont et al. 2001; Sako et al. 2003). These relativistically broadened emission lines are presumably emitted from the accretion disk, similar to the relativistically broadened Fe Kα emission line.

For Seyfert 1 galaxies there is in addition to the continuum described above a wealth of absorption lines from very lowly ionized ions (Si IV) to nearly completely ionized

ions (Fe XXIV). The absorption lines are all blueshifted, indicating that the absorption occurs in an outflow. In the UV band, where higher spectral resolution is obtained, these absorption lines often have several different velocity components, indicating that there are several kinematic components. The location of the narrow absorption line region is still uncertain, with estimates ranging between < 0.1 pc (Reeves et al. 2004) and 300 pc (Behar et al. 2003) for NGC 3783.

In the optical, UV and X-ray band of the spectrum we detect narrow emission lines emitted at the narrow line region (NLR) and broad emission lines emitted at the broad line region (BLR). The narrow emission lines are ten times broader than the narrow absorption lines, the broad lines are ten times broader than the narrow emission lines. The ionization range of the broad and narrow emission lines is significantly smaller, at least in the well studied case of NGC 5548, than the range observed for the narrow absorption lines. The narrow emission lines are probably formed at a different location than the narrow absorption lines or the broad emission lines. The NLR is generally extended (several lightmonths) and is fragmentary in shape (Ulvestad, Wilson & Sramek 1981). The size of the BLR can be determined using reverberation mapping, and has a size of a few light days to a lightmonth (Peterson & Wandel 2000).

1.4 Cartoon models for the core of an AGN

The X-ray observations as well as those in the optical, radio and infrared can be explained by two different models describing the inner parsecs of an AGN. Both models unify the unobscured and obscured AGNs by invoking different viewing angles. The first model is based on optical and infrared observations (Antonucci & Miller 1985; Urry & Padovani 1995); the second model, by Elvis (2000), is based on X-ray and UV observations.

1.4.1 Standard model

The standard model is depicted in Fig. 1.1. In the center is the SMBH with its accretion disk and surrounded by a donut shape torus in the equatorial plane. However, other geometries for this torus are also possible, see Chapter 1.3. Thus if we look directly at the accretion disk, i.e. an inclination angle smaller than about 60°, then the object is classified as a Seyfert 1 galaxy. For Seyfert 2 galaxies we look directly at the torus, which absorbs the continuum emission from the accretion disk. The inclination angle is thus between 60° and 90°, however, the exact range depend on the opening angle of the torus. In a cone along the polar directions there is a hot outflowing wind accelerated by radiation pressure. Embedded in this wind are two types of clouds. Those
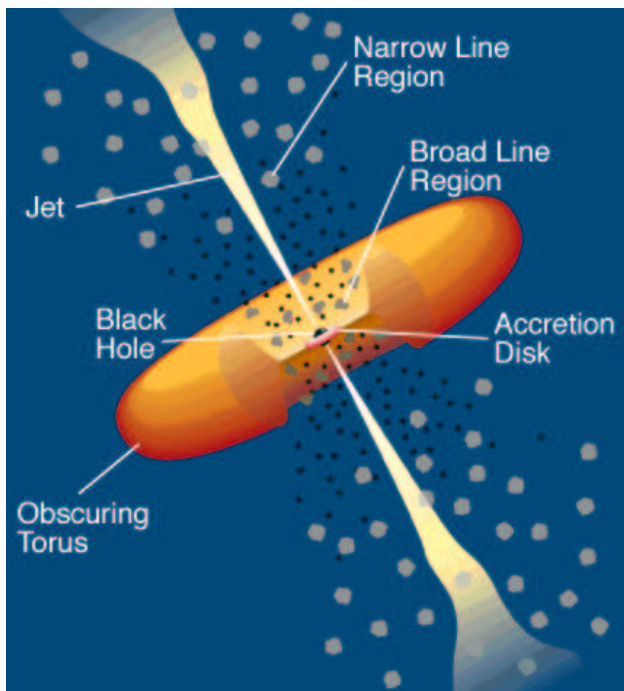
Figure 1.1: The standard model for the unification of AGN. For a Seyfert 1 galaxy one looks directly at the accretion disk, while for a Seyfert 2 galaxy one looks through the torus, here labeled obscuring torus. From Urry & Padovani (1995).

clouds close to the black hole emit broadened emission lines, those farther away emit the narrow emission lines. The broadening of these emission lines is due to Keplerian motion around the SMBH. These clouds are generally assumed to be in pressure equilibrium with the hot outflowing wind, as otherwise they will disintegrate (Krolik & Kriss 2001). However, other confinement mechanisms, such as magnetic confinement are also possible. These clouds could form from the irradiated inner edge of the torus, or from the accretion disk. The location of the narrow absorption lines is not specified, but probably the narrow absorption lines are formed in clouds embedded in the outflow.

1.4.2   Model by Elvis

The model by Elvis (2000) is depicted in Fig. 1.2. In the center is the SMBH and the accretion disk. Starting from an instability on the accretion disk there is an outflow in the form of a narrow stream. This outflow is bent and accelerated due to radiation pressure. As the outflow is bent, there is a large range of inclination angles for which absorption from this outflow can be seen. Depending on where the line of sight intersects this outflow, narrow absorption lines (close to the SMBH) or broad absorption lines as detected in broad absorption line quasars (far from the SMBH) are produced. The broadening of these absorption lines is due to the non-collimation of the outflow and not due to Keplerian rotation. The broad emission line clouds are carried along in the flow with which they are in pressure equilibrium. The broadening of these clouds is due to Keplerian rotation, similar to the standard model. In this model no torus is specified, as the outflow itself absorbs the continuum emission. However, an equatorial torus is not excluded.

One can generalize this this model to have several outflows to explain the different kinematic components observed in the UV band. In the Elvis model the clouds are in pressure equilibrium within an outflow. However, in a more general model this is not a prerequisite. An alternative is that the stream expands as it moves outward, and that there is a density gradient orthogonal to the outflow. This density gradient results in a gradient in the ionization of the gas.

1.4.3   Comparison between the models

The main difference between the models is the viewing angle one predicts is necessary to observe a Seyfert 1 or a Seyfert 2 galaxy. In the standard model if the disk is observed face on then the AGN is classified as a Seyfert 1 galaxy, if observed edge on, through the torus, it is classified as a Seyfert 2 galaxy. In the model by Elvis, Seyfert 1 galaxies which have warm absorbers are observed if the inclination angle of the disk is between $\sim 60^{\circ}$ and 90°.

Both models predict a warm absorber with a few ionization states, but a generalized Elvis model could explain a warm absorber with a continuous ionization range. There is observational evidence (Chapter 5) that at least some of the absorbing clouds cannot be in pressure equilibrium with the hot outflow. Thus some other form of confinement, such as magnetic, is necessary for a cloud model. Both models have a problem explaining the several, well separated outflow velocities observed for most UV absorption lines (Crenshaw et al. 1999). These velocity components are stable over timescales of decades, and only small velocity variations have been observed (Gabel et al. 2003). One of these kinematic components is present over an ionization range from C IV to
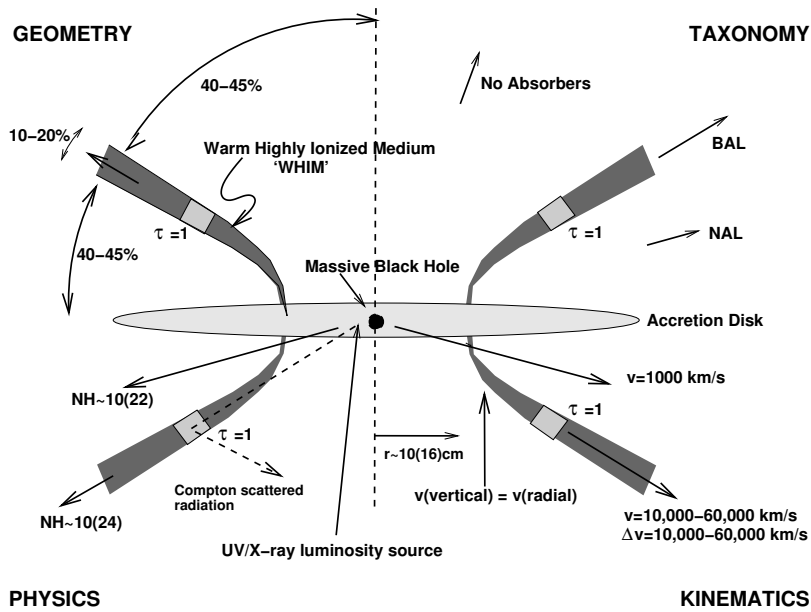
Figure 1.2: The model by Elvis (2000), where the outflow is in the form of narrow streams rather than a cone. The outflow is bent due to radiation pressure, and the narrow and broad absorption lines and broad emission lines are formed in this outflow.

Si XIII (Chapter 5). It seems improbable that clouds with different ionization parameters have the same outflow velocity, while clouds with the same ionization parameter have different outflow velocities. These different outflow velocities and their stability are more naturally explained in a generalized Elvis model.

In a generalized Elvis model one can explain the different outflow velocities by outflows formed at different distances. However, with time, radiation pressure will merge the different outflows (Proga, private communication). Assuming steady state accretion, then from the observed ionization parameters and the outflow velocity we conclude that the outflow has a small opening angle (Chapter 4). These narrow outflows are inconsistent with the ionization cone presented in the standard model.

Some observations cannot be explained by either model. From UV spectra cross-correlation results between different epoch spectra the minimum number of broad line clouds can be estimated. In the case of NGC 4151 the number of clouds estimated

is about an order of magnitude more than the number of clouds calculated the size of the BLR, R, the covering factor, C, and the size of the clouds, r: $N = 4CR^2/r^2 = 2\times10^5 LU^{-4}$ with L the luminosity in 10^{46} erg s $^{-1}$ and U the ionization parameter (Arav et al. 1998). This casts doubt on the cloud model for broad emission lines. In 3C273 a jet and broadened emission lines (Sellgren et al. 1983) are observed, which seems to indicate that the broad emission line clouds have a rotational plane perpendicular to the jet, or have chaotic instead of Keplerian motions.

1.5   Wind models

The measured blueshift of the UV absorption lines led to the conclusion that the absorbing gas is in the form of an outflow (Crenshaw et al. 1999). Several mechanisms for accelerating this outflow have been proposed, from gas pressure to magneto-centrifugal force and radiation pressure. The main problem for all these models is to explain why the gas is not fully ionized. The radiation field from the accretion disk and the comptonized photons is such that unless shielding occurs, the gas should be completely ionized. For this reason many models predict that the outflow has to be in the form of clouds, where there is a density gradient. Another possibility is that the outflow is somehow shielded, leading to an attenuated radiation field at the origin of the outflow.

If the wind is driven by line radiation pressure, then the wind is shielded by the X-ray opacity, and the wind itself has a density gradient resulting in a continuous ionization range (Proga, Stone & Kallman 2000). The radiation driven wind models indicates that a self-shielded wind can be launched from a radius $\leq 10^{14}$ m. The ratio of X-ray to UV opacity determines the outflow velocity. For a large ratio there will be a fast outflow, such as observed in broad absorption line quasars. For a small ratio a slow wind is created, as the radiation is nearly completely shielded by the X-ray gas resulting in a lessening of the line driving force. This slow wind is observed as the warm absorber in Seyfert 1 galaxies. These predictions are consistent with the observation that the soft X-ray luminosity is anti-correlated with the width of the C IV UV absorption line (Proga, Stone & Kallman 2000).

In all wind models most of the gas is completely ionized. In the radiation driven winds, the wind is bent due to radiation pressure, and is close to the accretion disk, while the regions near the poles are of low density and completely ionized. For the slow winds, as observed in Seyfert 1 galaxies, the radiation driven wind models predict a column density N_H of around 10^{28} m^{-2}. From the ionized X-rays spectra detailed in this thesis we find a N_H around 10^{27} m^{-2}, excluding completely ionized gas. From the line driven radiation pressure codes one predicts an asymmetric shape for the absorption lines, which has been confirmed by high resolution, high signal to noise UV

observations of Mrk 279 (Arav et al. 2004). These results make the radiation driven outflow models highly attractive to describe the real outflows occurring in the AGN's.

1.6 Spectral diagnostics

Using high resolution spectroscopy one can determine plasma properties such as ionization, temperature, velocities and abundances. The physical processes dominant in the ionization of the plasma, such as photoionization or collisional ionization can be determined from line ratios and radiative recombination lines. The advantage of high resolution X-ray spectroscopy is the availability of many atomic transitions that have detectable spectral lines. In particular, we observe many transitions from O and Fe, but also transitions from C, N, Ne, Na, Mg, Si, S, Ar and possibly Ca and Ni. These many transitions allow for elemental abundance determinations. In the studied wavelength range of 1.5 Å to 100 Å lines from neutral O I to highly ionized Fe XXVI have transitions. This allows for an accurate determination of the ionization parameter or temperature of the plasma. In AGN photoionization is dominant, and we will focus on this process in the rest of this section.

1.6.1 Determination of the ionization state

In photoionization equilibrium, the plasma conditions are determined by solving two equations: energy balance (heating versus cooling) and number density balance (recombination versus ionization). For a low density ($n < 10^{14}$ m^{-3}) thin slab, the equilibrium conditions are primarily determined by the shape of the spectral energy distribution (SED) and the so-called ionization parameter ξ, defined by $\xi = L/nr^2$, where L is the luminosity, n the density and r the distance from the ionizing source. Assuming a spectral energy distribution (SED) we know the range of ionization parameters for which a certain ion is created. Thus the column densities measured for the different ions determine the ionization parameter. However, differing elemental abundances can complicate this determination. Only for iron do we detect enough ions, from lowly ionized Fe VI to highly ionized Fe XXVI to determine the ionization parameters independently of elemental abundances. In Fig. 1.3 the ionization parameter for the different observable iron ions is shown. Obtaining the ionization parameters from iron allows for the determination of elemental abundances of the other elements relative to iron. However, in practice some iron ions are heavily blended, complicating this method. In general all transitions from the different ions are used to determine the ionization parameters. Because hydrogen doesn't have absorption lines in the X-ray band, the elemental abundances are in general given relative to oxygen or iron.
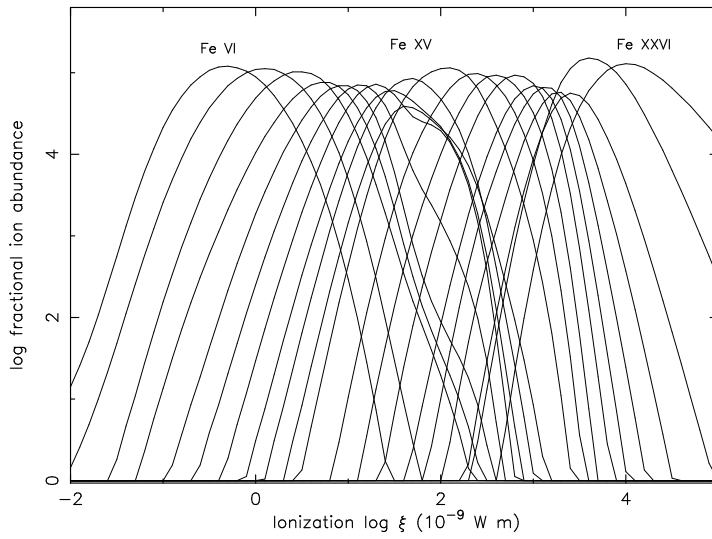
Figure 1.3: The fractional ion abundance versus ionization for Fe VI to Fe XXVI. The hydrogen abundance is 10 in this scale.

An important question is whether there are discrete ionization components, or whether the ionization has more continuous distribution. In this thesis we use both hypotheses. For the continuous ionization model the total hydrogen column density is derived from photoionization models for each individual ion. This hydrogen column density is then plotted against the ionization parameter for which the ion has its maximum column density. Consistency of the assumed continuous ionization distribution with the derived column densities shows then whether this model is appropriate or not. A more elegant method is to assume two extreme ionization parameters with a parametrized ionization distribution function and apply this model directly to fit the observed spectra. With this method we correctly take into account that an ion is formed over a range in ionization parameter.

An absorption model has been generated (Chapters 4 and 5) to test whether the distribution of column density versus ionization parameter is not continuous but discrete, with multiple different discrete ionization parameters. The model is the sum of individual components with only the ionization parameters and column density as free parameters. As many such components are added as necessary to obtain a good fit to the data. In general we need $2 - 5$ such components. All models depend on

10

the input SED and on the photoionization code used to obtain the ionization balance. However, differences in the SED or photoionization code have only a limited effect, mostly compressing or stretching the ionization scale.

1.6.2 Velocity broadening

In the X-ray band we observe several line series which allow for accurate velocity broadening and column density measurements. If the optical depth is small the equivalent width of the line gives the column density for the ion. However, if the line has a substantial optical depth, then the measured width of the line is a measure for both the column density and the velocity broadening. For the stronger lines, the optical depth is in general rather large, but the higher order lines in the line series or transitions with lower oscillator strengths do allow to separate the column density effect from the velocity broadening and measure both. The velocity broadening is a measure for the turbulent (and in some models the thermal) velocity fields. In the models where the ionization parameter or temperature is a free parameter, the thermal velocity is included in the modeling and the velocity width is an indication of turbulence.

1.6.3 Accuracy of atomic data

The above diagnostics are highly dependent on the availability of accurate atomic data such as wavelength and oscillator strength. For most of the stronger spectral lines and the Ly series these atomic data are well known. However, for some lines the calculated wavelength is not accurate, sometimes with errors similar to the full width half maximum (FWHM) resolution of the LETGS instrument. This is due to the difficulty of producing these ions in laboratory experiments. The O v absorption line at 22.374 Å, is a good example of a strong line where the calculated wavelength was inaccurate by 0.044 Å (see Chapters 4 and 5). The wavelength of this line was measured with the Electron Beam Ion Trap, which produces highly charged ions in a laboratory setting (Schmidt et al. 2004). Also for the O ii line at 23.33 Å the calculated wavelength differs significantly from the one measured with the HETGS (Juett et al. 2004). For the stronger lines a mismatch is easily detected in high signal to noise ratio spectra, but for the many weaker lines the difference is harder to detect and correct. As we need to self-consistently model all the spectral lines present in the spectrum, these errors could potentially propagate into the determined ionization parameter or abundance. The oscillator strengths in general agree between the different calculations to about 10 %.

Another possible source of error is that certain recombination processes are not correctly included, which can lead to errors in the photoionization equilibrium calculations. For the lower ionized iron ions the dielectronic recombination rates used in

the atomic data calculations are inaccurate (Netzer et al. 2003; Kraemer, Ferland & Gabel 2004; Netzer 2004). As a result the calculated ionization for these ions is too low. As iron is very important in the ionization parameter determination this can cause systematic errors in the ionization parameter.

1.7 This thesis

The launch of the *Chandra* and XMM-*Newton* satellites allowed for the first time high resolution X-ray spectroscopy of the brighter extragalactic X-ray sources sources. In this thesis we take advantage of the high resolution to study Seyfert 1 galaxies and a quasar, and in particular their ionized winds.

In Chapter 2 we describe the instruments used to obtain the spectra and the statistical methods used in the analysis of these spectra. In Chapter 3 we describe the *Chandra* LETGS and XMM-Newton spectra obtained for NGC 4593. In the spectra we only detect weak lines from highly ionized gas and lowly ionized gas, and not a standard warm absorber. An important question discussed in this thesis is the geometry and the physical conditions of the outflows observed through absorption lines. Is this outflow in the form of clouds which are in pressure equilibrium within a hot medium, or are these outflows in the form of narrow streams? In the first model the outflowing gas can only have a few particular ionization values, depending on the SED assumed. In the second scenario there is a density gradient that results in a continuous ionization structure. Both scenarios are extensively discussed in Chapters 4 and 5. Another question discussed in Chapter 5 is whether these outflows escape the galaxy to enrich the inter galactic medium (IGM), or fall back onto the accretion disk of the host galaxy. In Chapter 6 we study in detail the broad emission lines observed in the X-ray and UV spectra of NGC 5548, and model these with the photo-ionization codes CLOUDY and XSTAR. In Chapter 7 we discuss the heavily absorbed spectrum of IC 4329A, for which we detect absorption from the host galaxy as well as from the warm absorber close to the core. The ionized absorption from the IGM itself was studied by using the quasar Ton 1388 (Chapter 8) to illuminate this gas.

References

Antonucci, R. R. J. & Miller, J. S., 1985, ApJ, 297, 621

Arav, N., Barlow, T. A., Laor, A., et al., 1998, MNRAS, 297, 990

Arav, N., Gabel, J., Scott, J., et al., in preparation

Barthel, P. D., 1989, ApJ, 336, 606

Behar, E., Rasmussen, A. P., Blustin, A. J., et al., 2003, ApJ, 598, 232

Branduardi-Raymont, G., Sako, M., Kahn, S. M., et al., 2001, A&A, 365, L140

Chakrabarti, S. K. & Titarchuk, L. G., 1995, ApJ, 455, 623

Crenshaw, D. M., Kraemer, S. B., Boggess, A., et al., 1999, ApJ, 516, 750

Elvis, M., 2000, ApJ, 545, 63

Gabel, J. R., Crenshaw, D. M., Kraemer, S. B., et al., 2003, ApJ, 595, 120

Guilbert, P. W. & Rees, M. J., 1988, MNRAS, 233, 475

Iwasawa, K., Fabian, A. C., Reynolds, C. S., et al., 1996, MNRAS, 282, 1038

Juett, A. M., Schulz, N. S. & Chakrabarty D., 2004, in press

Königl, A & Kartje, J. F., 1994, ApJ, 434, 446

Kraemer, S. B., Ferland, G. J., Gabel, J. R., 2004, ApJ, 604, 556

Krolik, J. H. & Kriss, G. A., 2001, ApJ, 561, 684

Lightman, A. P. & White, T. R., 1988, ApJ, 335, 57

Nenkova, M., Ivezić, Ž. & Elitzur, M., 2002, ApJ, 570, L12

Netzer, H., Kaspi, S., Behar, E., et al., 2003, ApJ, 599, 933

Netzer, H., 2004, ApJ, 604, 551

Peterson B. M. & Wandel, A., 2000, ApJ, 540, L13

Proga, D., Stone, J. M. & Kallman, T. R., 2000, ApJ, 543, 686

Proga, D., 2003, private communication

Reeves, J. N., Nandra, K., George, I. M., et al., 2004, ApJ, 602, 648

Röttgering, H., Jaffe, W., Meisenheimer, K., et al., 2004, Proc. SPIE, Ed. Traub, W. A., Vol. 5491, 9

Sako, M., Kahn, S. M., Branduardi-Raymont, G., et al., 2003, ApJ, 596, 114

Schmidt, M., Beiersdorfer, P., Chen, H., et al., 2004, ApJ, 604, 562

Schödel, R., Ott, T., Genzel, R., et al., Nature, 419, 694

Sellgren, K., Soifer, B. T., Neugebauer, G. & Matthews, K., 1983, PASP, 95, 289

Seyfert, C. K., 1943, ApJ, 97, 28

Shakura, N. I., & Sunyaev, R. A., 1973, A&A, 24, 337

Tanaka, Y, Nandra, K., Fabian, A. C., et al., 1995, Nat. 375, 659

Ulvestad, J. S., Wilson, A. S. & Sramek, R. A., 1981, ApJ, 247, 419

Urry, C. M. & Padovani, P., 1995, PASP, 107, 803

Wilms, J., Reynolds, C. S., Begelman, M. C., et al., 2001, MNRAS, 328, 27